Journal of Catalysis **185,** 393–407 (1999)
Article ID jcat.1999.2511, available online at http://www.idealibrary.com on IDEAL®

Acetone and Acetaldehyde Oligomerization on TiO_2 Surfaces

Shengcheng Luo and John L. Falconer

Department of Chemical Engineering, University of Colorado, Boulder, Colorado 80309-0424

Received December 2, 1998; revised March 31, 1999; accepted April 2, 1999

Acetone undergoes aldol condensation and cyclization reactions on TiO_2 to form mesitylene (1,3,5-trimethylbenzene) below 400 K. The reaction rate is slow on pure anatase TiO_2, but on Degussa P25, a mixture of anatase and rutile, more than 20% of a monolayer of acetone forms mesitylene during temperature-programmed desorption or hydrogenation. Other C_5–C_9 hydrocarbon products also form on both oxidized and reduced TiO_2, whereas hexene forms only on reduced TiO_2. Acetaldehyde undergoes aldol condensation on both types of TiO_2; acetaldehyde either desorbs or forms dimeric condensation products on anatase. However, on Degussa P25 TiO_2, trimeric condensation products, higher molecular weight compounds, and coke also form. In addition, C_5H_8, C_5H_{10}, C_6H_{10}, and C_9H_{14} form as secondary reaction products of aldol condensation. Surface concentrations of acetaldehyde and acetone are higher on Degussa P25 than on anatase TiO_2. Degussa P25 has more sites that catalyze aldolization, and it has more acid sites. These condensation reactions, which take place at relatively low temperature, may be partly responsible for deactivation of Degussa P25 during photocatalytic oxidation.

INTRODUCTION

Idriss *et al.* (1, 2) have investigated the reactions of acetaldehyde on TiO_2 surfaces for both single crystals and powders using temperature-programmed desorption (TPD). They observed three reactions for acetaldehyde on the TiO_2(001) surfaces: reduction to ethanol, aldol condensation to crotonaldehyde and crotyl alcohol, and coupling to butene. Reduced surfaces were active for coupling to form butene due to the presence of oxygen vacancies, and oxidized surfaces were active for aldolization to crotonaldehyde and crotyl alcohol due to the abundance of oxide anions acting as Lewis base sites. On anatase powder, crotonaldehyde was produced with high selectivity. Idriss *et al.* [3] also studied the reactions of acetaldehyde on CeO_2 and observed the formation of acetone in addition to crotonaldehyde, crotyl alcohol, butene, butadiene, and ethanol. They proposed that acetaldehyde was oxidized to acetate on the CeO_2 surface, and then acetone was formed via acetate ketonization.

Idriss *et al.* (1, 2) reported the formation of only the dimeric condensation products of acetaldehyde (crotonaldehyde and crotyl alcohol) on both single crystal (001) and anatase TiO_2. Further aldol condensations of acetaldehyde have been reported, however, on other oxide surfaces (4). We recently reported (5) that acetaldehyde undergoes aldol condensation on Degussa P25 TiO_2 to form crotonaldehyde, but in addition, further condensation forms larger aldehydes such as hexan-2,4-dienal. Idriss *et al.* (1, 2) observed that most of the acetaldehyde adsorbed on their TiO_2 formed gas phase products during TPD. Similarly, on rutile and anatase TiO_2, Rekoske (6) observed that 95% of adsorbed acetaldehyde formed gas phase products during TPD (for samples without prereduction). In contrast, on Degussa P25 TiO_2 a much smaller fraction of a monolayer of acetaldehyde desorbed during TPD or TPH (temperature-programmed hydrogenation) (5, 7). Instead, larger molecules formed that were bound to the surface even at high temperatures. Degussa P25 is reported to be a mixture of anatase and rutile, but it has different catalytic properties from either of these pure phases.

Larson and Falconer (8) reported that acetone was weakly adsorbed on Degussa P25 TiO_2 and desorbed intact, though they did not look for higher molecular weight compounds. Similarly, Brinkley and Engel (9) observed that acetone desorbed intact from TiO_2(110). Thus, in contrast to the behavior of acetaldehyde, no studies have reported that acetone undergoes condensation reactions on TiO_2.

The formation of these larger molecules on Degussa P25 TiO_2 is of interest because it is a superior catalyst for photocatalytic oxidation (PCO) of volatile organic compounds (3, 10–15). However, as with most catalysts, deactivation is a concern, and recent studies (13) showed that TiO_2 rapidly deactivates during PCO of acetaldehyde at 363 K. Because the catalyst also deactivated in the absence of UV light at 363 K, a dark reaction appeared to be responsible for deactivation. Acetaldehyde apparently forms surface poisons at 363 K faster than they can be oxidized photocatalytically. The TiO_2 probably also deactivates below 363 K, though at a slower rate. Since the aldol condensation also take places at moderate temperatures, deactivation may be due to growth of larger molecules on the TiO_2 surface. Since these reactions occur to a much smaller extent on model surfaces such as single crystals and pure anatase powders, it is important to study them on the same catalysts that are active for PCO.

0021-9517/99 $30.00

The nonphotocatalytic reactions of acetaldehyde, besides being of interest for acetaldehyde PCO, may take place during PCO of ethanol on TiO_2 since acetaldehyde forms as an intermediate (7, 10–12). Moreover, when acetaldehyde reacted on TiO_2 at elevated temperatures, it poisoned PCO sites that favored complete oxidation of ethanol (10). Thus, the poisoned catalyst was much more selective for partial oxidation of ethanol to acetaldehyde. If poisoning is due to acetaldehyde condensation, then the same sites that catalyze acetaldehyde condensation may be responsible for PCO activity. A better understanding of what reactions take place on these sites might allow us to improve TiO_2 photocatalysts. Similarly, the reactions of acetone on TiO_2 are of interest since acetone forms as a partial oxidation product of 2-propanol during PCO (8), and PCO of acetone has been studied (16, 17).

The objective of the current study is to determine the extent of acetone and acetaldehyde oligomerization on Degussa P25 TiO_2. For comparison, these oligomerization reactions were also carried out on anatase TiO_2 from American Instruments Co. Idriss *et al.* (2) used this TiO_2 in their studies. Both oxidized and reduced forms of the two TiO_2 catalysts were used since aldol condensation of acetaldehyde was reported to take place more readily on oxidized TiO_2(001) surfaces, whereas reductive coupling occurred preferentially on reduced TiO_2 (1). Acetaldehyde oligomerization to form the trimer, hexan-2,4-dienal, on oxidized Degussa TiO_2 was reported in our recent study (5).

We observe that acetone undergoes condensation reactions on Degussa P25, but not to a significant extent on anatase TiO_2. Acetone undergoes aldol condensation on $MgO–Al_2O_3$ and other oxides (18, 19). Besides the principal products formed from two and three acetones (diacetone alcohol, mesityl oxide, phorone, and isophorone), Reichle (18, 19) observed many transient intermediates. He proposed that aldol condensation of acetone and further condensation of these products with acetone formed these compounds. Lippert *et al.* (20) also investigated the aldolization reactions of acetone over solid base catalysts such as $Ca(OH)_2$, $La(OH)_3$, ZrO_2, and CeO_2 in the vapor phase. The more basic the catalyst, the higher the yield of mesityl oxide and isophorone; mesitylene (1,3,5-trimethylbenzene) formation from condensation and cyclization of three acetones was favored with decreasing basic strength. They proposed that the trimeric and tetrameric condensation products crack to form C_7 and C_{10} products plus acetic acid.

Temperature-programmed desorption, hydrogenation, and oxidation (TPD, TPH, TPO) were used in the current study to identify species that form on the surface from oligomerization reactions. Some oligomers may form at low temperatures and may be poisons for PCO, but they may not desorb until much higher temperatures during TPD or TPH. Since acetaldehyde can form strongly bound, unsaturated species, TPH was used in an attempt to hydrogenate these surface species to more weakly bound molecules that desorb. Thus, the objective was to use TPH to remove more surface species than could be removed during TPD. Hydrogen pressure above atmospheric was used to increase the rate of hydrogenation. Titania is not a good hydrogenation catalyst, but it hydrogenates organics at elevated temperature (21, 22). Furthermore, the mass spectrometer sensitivities of some species increase when H_2 is used as a carrier gas instead of He. For example, the sensitivity of CO_2 and CO with H_2 carrier gas is about three times higher than with He carrier gas. Temperature-programmed oxidation was used after TPH or TPD to determine the amount of carbon-containing species remaining on the surface; these surface species oxidize to CO_2 during TPO even if they are not removed during TPH. The total amount of acetaldehyde originally adsorbed on the TiO_2 was also measured by TPO. The TiO_2 surfaces were further characterized by TPD of pyridine and CO_2 to provide some measure of the number of acidic and basic sites (23–25).

In addition to the interest in these reactions for PCO, the formation of larger molecules from aldehydes and ketones is important industrially. Condensation reactions form numerous chemicals such as mesityl oxide, diacetone alcohol, phorone, mesitylene, isophorone, and 2-ethylhexenal, which are frequently hydrogenated to yield solvents and plasticizers, such as methyl ethyl ketone, 3,5-xylenol, and 2,3,5-trimethylphenol (4, 18–20, 26–32).

EXPERIMENTAL METHODS

Reactions of acetone and acetaldehyde were carried out on two types of TiO_2, Degussa P25 and anatase from American Instrument Co (AIC). The Degussa P25 TiO_2 has been reported to be a mixture of $75 \pm 5\%$ anatase and $25 \pm 5\%$ rutile and to contain less than 0.5% impurities (SiO_2, Al_2O_3, and trace amounts of Fe_2O_3) (33). Its BET surface area is 50 m^2/g, and it is produced by flame hydrolysis of $TiCl_4$ at temperatures above 1473 K in the presence of O_2 and H_2. The impurities were not detected on the surface of Degussa P25 in a previous analysis by XPS (34). The TiO_2 from AIC is a pure anatase phase free of rutile according to XRD patterns, and it has a BET surface area of 10.3 m^2/g (35).

A packed-bed, tubular reactor (7 mm i.d.) was used for temperature-programmed desorption (TPD), hydrogenation (TPH), and oxidation (TPO). The reactor was made of quartz and had a quartz frit to support the catalyst. About 50 mg of Degussa TiO_2 or 120 mg of AIC TiO_2 was placed on quartz wool, which rested on the reactor frit, and additional quartz wool was placed on top of the catalyst bed. The temperature was measured with a chromel–alumel thermocouple placed in the center of catalyst bed. A temperature controller used feedback from the thermocouple to provide a constant temperature ramp of 1 K/s from room temperature to 723 K. The temperature

was not increased above 723 K if additional experiments were to be done on the TiO_2 sample because anatase undergoes a phase change to rutile at higher temperatures. The gas flow rate was 100 cm^3 (STP)/min. For TPD, pure He flow was used, for TPH, pure H_2 was used, and for TPO, a 20% O_2/80% He stream was used.

The effluent from the reactor was sampled by a Balzers quadrupole mass spectrometer through a silica capillary. A computer allowed the temperature and multiple mass peaks to be detected simultaneously. A back-pressure regulator downstream of the reactor was used to increase the reactor pressure and increase the pressure in the mass spectrometer chamber, and this increased the sensitivity. For TPH of acetaldehyde, the pressure was maintained at 3 atm, whereas TPH of acetone, TPD, and TPO were all carried out at ambient pressure.

To create a reproducible oxidized surface, the TiO_2 was oxidized in 20% O_2 at 723 K for 30 min before each experiment, and the flow was then switched to He and the TiO_2 cooled to room temperature. The flow was then switched to H_2 for TPH or kept in He for TPD. To obtain a reduced surface, the oxidized catalyst was held in H_2 at 723 K for 45 min.

The TiO_2 surface was saturated with acetaldehyde by injecting excess acetaldehyde gas upstream of the reactor at room temperature in H_2 flow. For a few experiments, the TiO_2 was exposed to acetaldehyde at 473 K. For acetone, liquid was injected and evaporated upstream of the TiO_2. Both acetaldehyde (99.5+%, Aldrich Chemical Company, Inc.) and acetone (99.6%, Fisher Scientific) were used without further purification. None of the products detected during TPD and TPH were seen in the acetaldehyde and acetone that was injected into the mass spectrometer for calibration. To identify the products observed during TPD and TPH, these compounds were either adsorbed on the TiO_2 (crotonaldehyde, mesitylene) or injected into the flow stream below the reactor to calibrate (2,3-dimethyl-2-butene (hexene), trans-2-methyl-1,3-pentadiene (hexadiene), benzene, toluene, ethylbenzene, *m*-xylene, etc). Carbon dioxide was adsorbed at 243 K and at room temperature, and TPD was then carried out from 243 to 473 K or from room temperature to 723 K. The TiO_2 was cooled by flowing cold N_2 gas around the outside of the reactor. Pyridine (99.9%, Aldrich Chemical Company, Inc.) was adsorbed at room temperature to saturation coverage by evaporation of the liquid.

RESULTS

Acetone on Oxidized Degussa TiO_2

Both the reactions observed and possible reactions of acetone during acetone TPH are summarized in Scheme 1. Though acetone condensation reactions have not been reported previously on TiO_2, acetone readily forms the

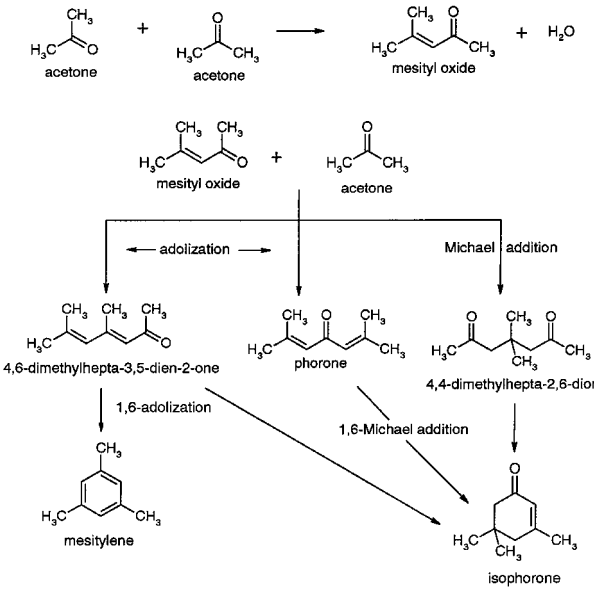

SCHEME 1

trimeric condensation and cyclization product mesitylene (1,3,5-trimethylbenzene) on Degussa TiO_2. As shown in Fig. 1, acetone desorbs intact at low temperature from an oxidized TiO_2 surface during TPH; half of the adsorbed monolayer desorbs intact. Acetone appears to be relatively weakly adsorbed, as reported previously (8), and desorbs with a peak temperature of 380 K. The other half reacts, mostly to form larger molecules. The mesitylene in Fig. 1 forms in two peaks centered at 435 and 670 K. The area under the mesitylene curve is much smaller than that for acetone, but mesitylene forms from three acetone molecules, so *22% of the acetone monolayer forms mesitylene*. Mass fragments at $m/e = 105$, 91, 79, 78, and 77 were compared to those from desorption of adsorbed mesitylene to verify

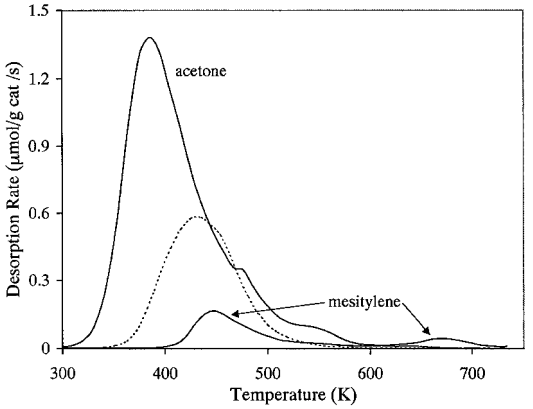

FIG. 1. Rates of formation of acetone and mesitylene during TPH of a monolayer of acetone adsorbed at 300 K on oxidized Degussa P25 TiO_2. Additional products are not shown for clarity. The dotted line is the desorption rate for saturated coverage of mesitylene at 300 K.

TABLE 1

Temperature-Programmed Hydrogenation of Acetone on TiO_2

TiO_2 surface	Acetone (C_3H_6O)	Mesitylene (C_9H_{12})	Hexene (C_6H_{12})	Hexadiene (C_6H_{10})	CO_2	CO	Other[a]	TPO
Degussa oxidized								
Amount[b]	354	141	—	10	4	15	~50	65
Percentage of monolayer	55	22		1.6	0.6	2.3	8	10
Degussa reduced								
Amount	360	109	7	30	2	13	~60	62
Percentage of monolayer	56	17	1.1	4.7	0.3	2.0	9	10
Anatase oxidized								
Amount	63	~1	—	—	0.6	2.4	~1[c]	1–2
Percentage of monolayer	91	1.4			0.9	3.5	1.4	2
Anatase reduced								
Amount	60	~1	—	—	0.2	15	~2[c]	1–2
Percentage of monolayer	90	1.4			0.3	2.2	3	2

[a] Includes C_5H_8, C_9H_{14}, C_9H_{16}, $C_{10}H_{16}$, and mesityl oxide.
[b] Amount in μmol carbon/g catalyst.
[c] Also includes C_6H_{10} and C_6H_{12}, in addition to the above species.

its identification. Adsorbed mesitylene desorbs with a peak temperature of 430 K (dashed curve in Fig. 1), which suggests that its formation at 435 K from adsorbed acetone is desorption limited. Thus, the condensation reaction takes place at lower temperature. A monolayer of mesitylene is 51 μmol/g TiO_2. The formation of mesitylene at 670 K must be limited by a surface reaction.

Smaller amounts of other products also form during acetone TPH, and their amounts and percentages of a monolayer are listed in Table 1. The CO and CO_2 form in broad peaks. The species identified as "other" are the various organics that form in small quantities. Their amount was determined by differences between the amount of acetone adsorbed and the amount of calibrated products plus unreacted acetone that desorbed. The acetone monolayer coverage (213 μmol acetone/g TiO_2) was determined from the breakthrough of acetone pulses. Note that these other species were not calibrated for because of their small amounts; only 8% of the acetone monolayer reacts to form them. They form mostly at higher temperatures, as shown by the dashed lines in Fig. 2. Mesityl oxide ($m/e = 98$, 83), the dehydrated dimeric aldolization product, starts desorbing near 350 K, so acetone aldolization takes place at low temperatures. Hexadiene (C_6H_{10}) ($m/e = 82$, 67, 41) and pentadiene (C_5H_8) ($m/e = 68$, 67) form in peaks with maxima near 650 K, but no hexene (2,3-dimethyl-2-butene, $m/e = 84$, 69) was observed.

Figure 3a shows the mass peaks that correspond to mesitylene formation. Note that the signals at $m/e = 79$ and 91 are not identical in shape to the other signals, but instead have a high temperature shoulder. This indicates that an additional species besides mesitylene desorbs. Additional TPH experiments suggest that these shoulders correspond to the formation of nonatriene or cyclononadiene, C_9H_{14} ($m/e = 122$, 107 (dashed line in Fig. 4)). Also forming in small quantities and not shown in the figures are nonadiene or cyclononene, C_9H_{16} ($m/e = 124$, 109), decatriene, $C_{10}H_{16}$ ($m/e = 136$, 121), and butene, C_4H_8. No fragments of phorone or isophorone ($m/e = 138$, 123) were detected.

During TPH, about 10% of the acetone monolayer reacts, through further aldol condensation or secondary reactions of aldolization products, to form species that are too strongly bound to the surface to be removed by desorption or hydrogenation by 723 K. These species are oxidized to CO_2 and CO during a subsequent TPO, however, and their amounts are indicated in Table 1.

TPD of acetone was also carried out on oxidized Degussa TiO_2 and the spectra are almost identical to the TPH

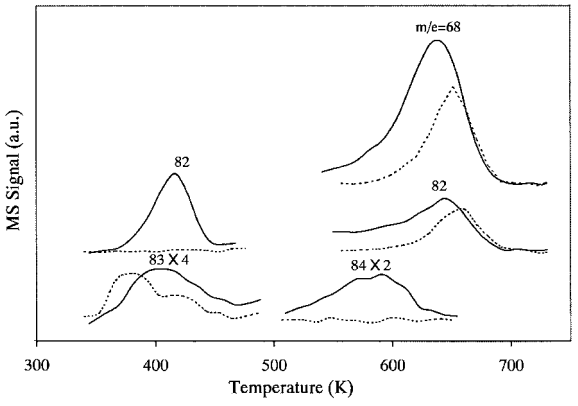

FIG. 2. Desorption of mesityl oxide ($m/e = 83$), hexene ($m/e = 84$), hexadiene ($m/e = 82$), and pentadiene ($m/e = 68$) during TPH of acetone on Degussa TiO_2 (uncorrected for mass spectrometer sensitivities). Dashed lines, oxidized TiO_2; solid lines, reduced TiO_2.

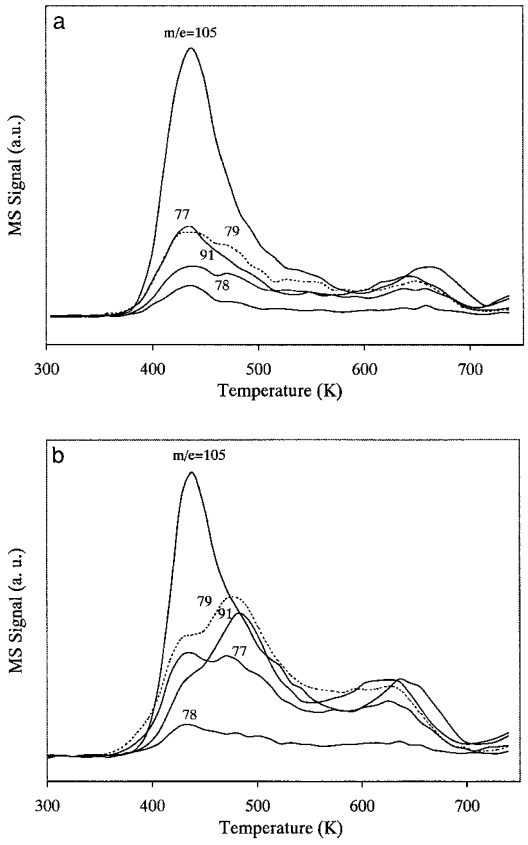

FIG. 3. Mass signals at $m/e = 105$, 91, 79, 78, and 77 during TPH of acetone on (a) oxidized and (b) reduced Degussa P25 TiO_2. Signals are not corrected for sensitivities.

spectra. The peak temperatures for each species are essentially the same, but the amounts detected during TPD are slightly smaller than those during TPH, and therefore, about 15% of the originally adsorbed carbon remains on the surface after TPD. Moreover, the mass spectrometer sensitivity was lower in He flow than in H_2 flow. Therefore, TPH increases the rate of formation of gas-phase species, but mainly increases detection sensitivity for products present in small concentrations.

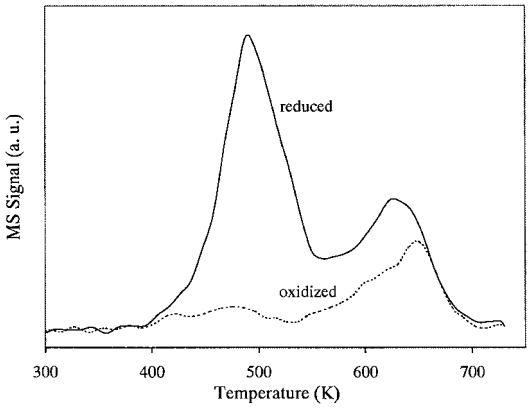

FIG. 4. Desorption of C_9H_{14} (nonatriene) during TPH of acetone on oxidized and reduced Degussa TiO_2.

Acetone on Reduced Degussa TiO_2

The TPH spectra on reduced Degussa TiO_2 (heated in H_2 at 723 K for 45 min) are similar to those on the oxidized surface. As shown in Table 1, less mesitylene forms on the reduced surface, but essentially the same amount of acetone desorbs. The amount of acetone adsorbed on the reduced surface (214 μmol/g TiO_2) is almost the same as that on the oxidized surface. Much more hexadiene forms on the reduced surface, and hexene also forms, whereas none was detected on the oxidized surface. As shown in Fig. 2 by the solid lines, 2,3-dimethyl-2-butene ($m/e = 84$, 69, 42, 41) forms in a peak at 580 K, and hexadiene ($m/e = 82$, 67, 41) desorbs in two peaks at 410 and 640 K. For the oxidized surface, fragments at $m/e = 79$ and 91 were seen as a small shoulder on the mesitylene peak in Fig. 3a, but $m/e = 79$ and 91 are larger peaks on the reduced surface in Fig. 3b and have maxima around 490 K. The presence of these peaks on the reduced surface verifies that nonatriene or cyclononadiene (C_9H_{14}) forms on both the oxidized and the reduced surfaces, with more forming on the reduced surface, as shown by mass fragment $m/e = 107$ in Fig. 4. More pentadiene (C_5H_8) and C_9H_{14}, but slightly less CO and CO_2, form on the reduced surface, as shown in Table 1. The amount of strongly bound species that are only removed by TPO is the same (10% of a monolayer) on the reduced and oxidized surfaces (Table 1).

Acetone on Oxidized Anatase TiO_2

The anatase TiO_2 has 20% of the surface area of Degussa TiO_2, but only 10% as much acetone adsorbs on the anatase TiO_2. That is, the acetone surface concentration on anatase TiO_2 is only half that on Degussa P25. The reactivity for acetone condensation is also quite different, as indicated by the amounts in Table 1. Only 1.4% of the adsorbed acetone condenses to form mesitylene and 91% desorbs intact. The TPH peak shapes for anatase TiO_2 are similar to those in Fig. 1, however. Acetone desorbs from both oxidized and reduced anatase with a peak temperature of 390 K, and mesitylene forms in a single small peak at 450 K, instead of the two peaks seen for Degussa TiO_2.

In contrast to Degussa TiO_2, most of the acetone that does not desorb intact from anatase TiO_2 reacts to form CO and CO_2. The selectivity for unsaturated species such as mesityl oxide, C_6H_{12}, C_6H_{10}, and C_9H_{14} is also low, only 1.4% for the oxidized anatase surface. The rate of C–C bond formation during TPH of acetone appears to be significantly lower on oxidized anatase TiO_2 than on oxidized Degussa TiO_2. Thus, only small amounts of high-molecular-weight compounds are produced via aldol condensation or reductive coupling. Consequently, following TPH only 2% of the

acetone remains on the surface as strongly bound products that are removed by TPO.

Acetone on Reduced Anatase TiO_2

The reduced and oxidized anatase TiO_2 exhibit similar reaction behavior; 90% of the acetone desorbs intact from the reduced surface. Slightly less acetone adsorbs (67 μmol/g TiO_2), and the same amount of mesitylene forms, but less CO_2 and CO form, as shown in Table 1. A small amount of C_9H_{14} desorbs with a peak at 500 K from the reduced surface. The selectivities for unsaturated species such as mesityl oxide, C_6H_{12}, C_6H_{10}, and C_9H_{14} are also low, only 3%, and are listed as "other" in Table 1.

Reduction of TiO_2

The desorption spectra of water *during TPH of acetone* on oxidized and reduced surfaces for each TiO_2 are shown in Figs. 5a and 5b. On the reduced surfaces (dashed lines) of both titanias, water desorbs in a broad peak from 350 to 550 K, whereas on the oxidized surfaces (solid lines), water also forms in a second, larger peak centered at 600–620 K. Since the second peak is seen only on oxidized TiO_2, it corresponds to H_2O formed from TiO_2 reduction, whereas the first peak is due to water formation from aldol condensation. The amounts of H_2O from reduction of oxidized Degussa and anatase TiO_2 are 209 and 70 μmol/g TiO_2, respectively. More oxygen is removed per nm^2 from anatase than from Degussa TiO_2, since the Degussa surface area is five times that of anatase. In addition, the water peak temperature for anatase is more than 20 K lower.

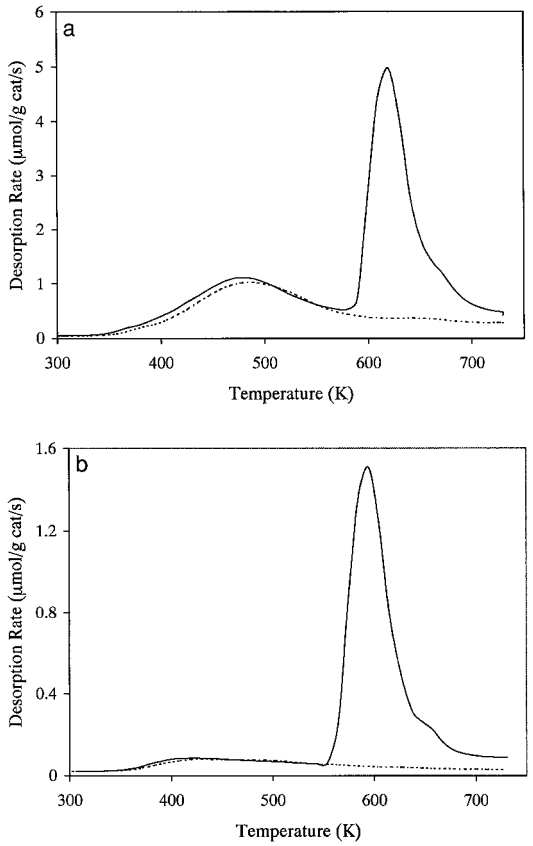

FIG. 5. Desorption rate of water during TPH of acetone in 1 atm H_2 for oxidized and reduced (a) Degussa TiO_2 and (b) anatase. The solid lines are for oxidized TiO_2 and the dashed lines for reduced TiO_2.

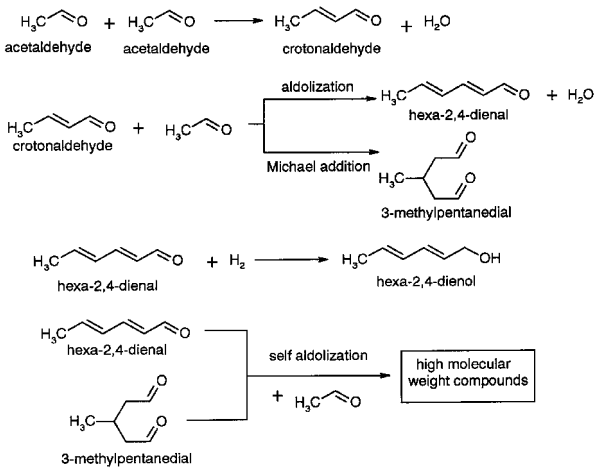

SCHEME 2

After systematically studying the stoichiometry of Degussa P25 TiO_2 with H_2 treatments from 523 to 773 K, Haerudin *et al.* (36) concluded that H_2 reduces TiO_2 with the formation of oxygen vacancies (Vo) and Ti^{3+} species:

$$Ti^{4+} + O^{2-} + H_2 \rightarrow H_2O + Vo + Ti^{3+} + e^- \qquad \Delta H = 183 \text{ kJ/mol.}$$

Matsuda and Kato also concluded that TiO_2 is easily reduced, but by a different reaction since the following reaction is only slightly endothermic [37]:

$$TiO_2 + H_2 \rightarrow Ti_3O_5 + H_2O \quad \Delta H = 8.9 \text{ kJ/mol.}$$

Acetaldehyde on Degussa TiO_2

We have already reported (5) that high-molecular-weight alkenes and alkylbenzenes form during TPH of acetaldehyde on oxidized Degussa TiO_2 via further aldol condensation. The same results were obtained on reduced Degussa TiO_2. The reactions are summarized in Scheme 2. As reported by Idriss *et al.* (1, 2) for TiO_2(001) and anatase TiO_2 surfaces, and shown in Fig. 6 for Degussa TiO_2, both acetaldehyde ($m/e = 29$) and crotonaldehyde ($m/e = 70$) desorb in peaks with maxima around 400 K, butene ($m/e = 56$) forms with a shoulder at 660 K and a peak that is not complete when heating is stopped, and butadiene ($m/e = 54$) forms in two peaks at 550 and 650 K. Water, CO, and CO_2 also form (not shown).

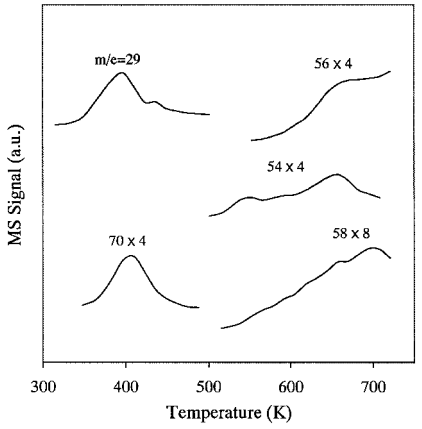

FIG. 6. TPH spectra for saturation coverage of acetaldehyde on Degussa TiO_2 (uncorrected for mass spectrometer sensitivities).

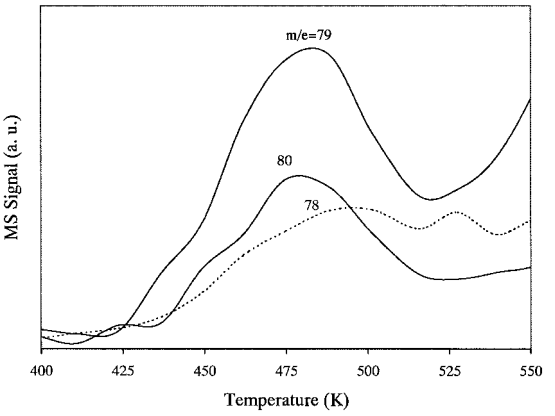

FIG. 8. Desorption of C_6H_8 and C_6H_6 during TPH of acetone on Degussa P25 TiO_2 (uncorrected for mass spectrometer sensitivities).

However, in contrast to results reported by Idriss *et al.*, larger molecules also form on Degussa TiO_2. The $m/e = 70$ fragment was used to identify crotonaldehyde. Idriss *et al.* (1) reported one peak at about 400 K, corresponding to crotonaldehyde desorption from {011}-faceted and {114}-faceted TiO_2(001) surfaces and from TiO_2 anatase powder. We observe two peaks at $m/e = 70$ from Degussa TiO_2: one at 410 K and the other at 670 K. In analogy to the Idriss *et al.* result, the peak at 410 K is assigned to crotonaldehyde. Although Idriss *et al.* (2) also observed a shoulder at 460 K and a peak at 560 K for $m/e = 70$ on TiO_2(001) that was not fully oxidized, they assigned both to crotonaldehyde. Our peak at 670 K is attributed to pentene desorption, however, because, as shown in Fig. 7, a fragment at $m/e = 55$ also has a maximum at 670 K, but the $m/e = 55$ signal is not seen at lower temperature. The signal at $m/e = 55$ is not from butene, since the $m/e = 56$ fragment has a different shape in Fig. 7. Pentadiene ($m/e = 68$, 67) also forms near 630 K.

As shown in Fig. 8, m/e fragments at 80, 79, and 78 are observed with maxima at 480 K. The peak shape of $m/e = 78$ is somewhat different from the others, and thus this group of peaks is assigned to two species: benzene C_6H_6 ($m/e = 78$) and hexatriene C_6H_8 ($m/e = 80$, 79). As reported before (5), hexan-2,4-diene-al ($m/e = 96$, 81, 79, 67, and 29), which is the trimeric condensation product of acetaldehyde, desorbs with a maximum near 600 K (Fig. 9). Another justification for the identification of hexan-2,4-dienal is the observation that hexan-2,4-dienol ($m/e = 98$, 83) desorbs at 670 K (Fig. 9). Aldol condensation of crotonaldehyde with acetaldehyde forms hexan-2,4-dienal, which is hydrogenated to hexan-2,4-dienol at higher temperature (Scheme 2).

At higher temperature, alkylbenzenes are also detected. As shown in Fig. 10, signals for fragments $m/e = 77$, 79, 91, 105, and 119 appear around 550 K, but do not reach their maxima by 723 K. These fragments might represent the following cations: phenyl (77), hexatrienyl (79), benzyl

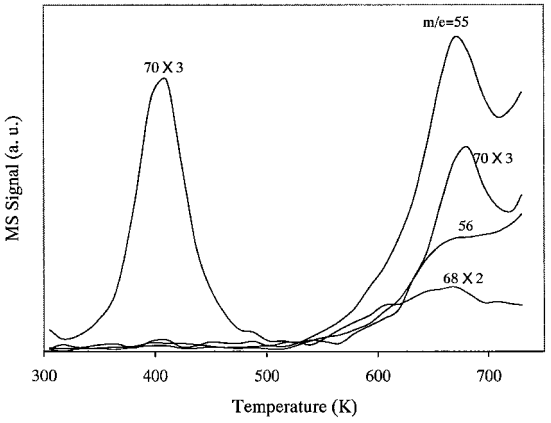

FIG. 7. Mass signals at $m/e = 70$, 68, 56, and 55 during TPH of acetaldehyde on Degussa P25 TiO_2 (uncorrected for mass spectrometer sensitivities).

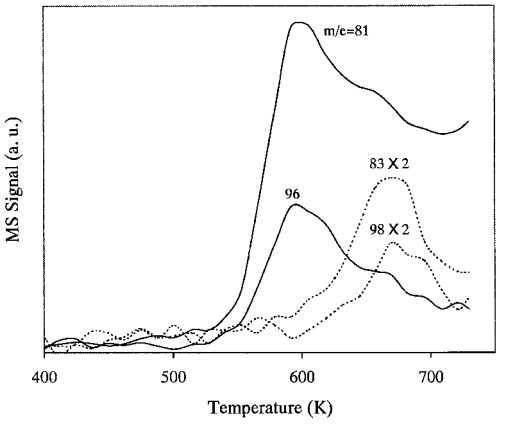

FIG. 9. Desorption of hexa-2,4-dienal ($m/e = 96$, 81) and hexa-2,4-dienol ($m/e = 98$, 83) during TPH of acetaldehyde on Degussa P25 TiO_2 (uncorrected for mass spectrometer sensitivities).

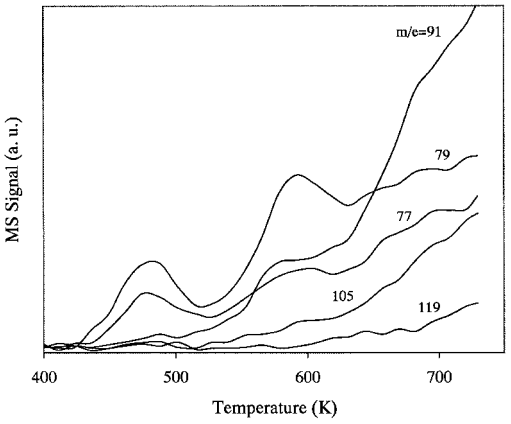

FIG. 10. Mass signals at $m/e = 119$, 105, 91, 79, and 77 during TPH of acetaldehyde on Degussa TiO_2 (uncorrected for mass spectrometer sensitivities).

(91), and phenylethyl or xylenyl (105), which are typically formed from various alkylbenzenes, such as toluene, xylene or ethylbenzene, and trimethylbenzene or methylethylbenzene. As evidence for the formation of high-molecular-weight compounds, small quantities of brown tars were sometimes observed on the bottom of reactor when it was removed from the furnace. These tars, with relative high boiling temperatures, formed during TPH and condensed at cooler parts of the reactor.

After TPH, TPO was used to determine the amount of carbon-containing species remaining on the surface and to estimate the H/C stoichiometry of the residue on the surface. The saturation coverage of acetaldehyde at room temperature is about 370 μmol/g TiO_2. More than 40% of the original carbon remains on the surface after TPH to 723 K, and the H/C stoichiometry of this species is 0.7. Surface species with H/C ratios of 0.5–1.0 are typical of coke (38), and the aromatic rings seen during TPH are also indicative of the formation of coke-type precursors. When TPD instead of TPH was carried out for acetaldehyde, 67% of the original carbon remained on the surface and was removed only by TPO.

Acetaldehyde Adsorption on Degussa TiO_2 at 473 K

Since the condensation reactions appear to take place at relatively low temperatures, acetaldehyde pulses were injected over Degussa TiO_2 at 473 K. As shown in Table 2, CO_2, CO, H_2O, and crotonaldehyde form, suggesting that continuous aldol condensation and other reactions take place at 473 K. During the subsequent TPD, almost all mass signals are larger than those observed for TPD after room temperature adsorption, especially those with high molecular weight, such as trimethylbenzene ($m/e = 120$, 106), ethylbenzene or xylene ($m/e = 106$, 91), toluene ($m/e = 92$, 91), and benzene ($m/e = 78$). Furthermore, more CO_2 and CO form during TPO after TPD than for adsorption at room temperature.

During the first injection at 473 K, most of the acetaldehyde converts to species that remain on the surface; only 17% of the injected acetaldehyde is observed intact and 3% oxidizes to CO_2 and CO. A large amount of water forms, but only a small amount of crotonaldehyde desorbs, probably because of further aldol condensation to form high-molecular-weight compounds, which do not desorb at 473 K. During subsequent injections, less H_2O, CO_2, and CO form as less acetaldehyde reacts, but more crotonaldehyde forms.

During the TPO after TPD to 723 K, species containing 1240 μmol carbon/g TiO_2 are detected. This amount of carbon is larger than the saturation coverage of acetaldehyde at room temperature (740 μmol carbon/g TiO_2). This result further confirms that high-molecular-weight compounds form through further aldol condensation of acetaldehyde on Degussa TiO_2.

Acetaldehyde on Anatase TiO_2

The TPH spectra for acetaldehyde adsorbed on oxidized anatase TiO_2 are almost the same as the TPD spectra reported by Idriss *et al.* (1) for the same TiO_2 preheated in He at 800 K for 2 h. Acetaldehyde and crotonaldehyde, the main products, desorb with peaks near 400 K. Butadiene, a minor product, forms in two peaks at 540 and 640 K. Water, and small amounts of acetone, CO, and CO_2 also

TABLE 2

Acetaldehyde Adsorption/Reaction at 473 K on Degussa TiO_2

Injection No.	Acetaldehyde	Crotonaldehyde	H_2O	CO_2	CO
Calibration	2640	0	0	0	0
1	445	13 (0.029)	778 (1.75)	122 (0.27)	91 (0.20)
2	1243	38 (0.031)	460 (0.37)	130 (0.10)	96 (0.08)
3	1165	37 (0.032)	288 (0.25)	101 (0.09)	78 (0.07)
4	1109	36 (0.032)	225 (0.20)	77 (0.07)	67 (0.06)
5	1646	52 (0.032)	236 (0.14)	53 (0.03)	50 (0.03)

Note. Data in amount (μmol/g TiO_2) and (ratio of amount to acetaldehyde unreacted).

desorb. However, in contrast to TPH of Degussa TiO_2, *no other species or fragment peaks are observed, except for a trace amount of butene (m/e = 56, 55).* Temperature-programmed oxidation indicates that only 4–5% of the original acetaldehyde remains on the anatase surface after TPH. This result is consistent with observations by Rekoske (6) on a similar anatase (Aldrich, 99.9+%; BET area, 10 m^2/g). He reported that only 5% of the acetaldehyde remained on his anatase TiO_2 (not reduced) after TPD. His saturation coverage was 37 μmol/g TiO_2, whereas we measure 50 μmol/g TiO_2. On his reduced anatase, Rekoske reported a 6% increase in the amount adsorbed, but the amount on the surface after TPD increased a factor of five to 22% of a monolayer. He also observed the formation of acetone and CO_2 on the oxidized TiO_2.

Acidity and Basicity of Titania

The TPD spectra for pyridine are shown in Fig. 11 for the two oxidized titania surfaces. Since the BET area of the Degussa TiO_2 is five times that of the anatase TiO_2, the TPD signal for the anatase is also presented multiplied by five for comparison. Pyridine desorbs in at three distinct peaks from the anatase TiO_2 at 400, 500, and 590 K. On Degussa TiO_2, the pyridine desorption spectrum is broader and distinct peaks cannot be identified, but by analogy to the anatase TiO_2, at least three peaks are probably present. Parrillo *et al.* (39) reported two peaks at about 390 and 730 K during TPD of pyridine on H-ZSM-5. They assigned the peak at low temperature to physically adsorbed pyridine, and the other peak to decomposition of pyridinium ion, which is the product of reaction between pyridine and surface Brønsted acid sites. Therefore, the first peak at 400 K on TiO_2 probably corresponds to physical adsorption of pyridine, and the other two peaks at higher temperature represent two types of sites with strong adsorption. Using IR, Rochester *et al.* (25, 40) concluded that pyridine interacts with rutile through either hydrogen bonds with surface hydroxyl groups or coordination with Lewis acid sites. Evacuation at 300 K removed the pyridine held by hydrogen bonds but not that on the Lewis acid sites. Other studies (41) of triethylamine adsorption on rutile also suggested two kinds of adsorption.

TABLE 3

Saturated Coverages of Pyridine and CO_2 on TiO_2

	Degussa TiO_2		AIC anatase	
Surface (ads. temp)	CO_2	Pyridine	CO_2	Pyridine
Oxidized (300 K)	4.4 (0.09)	262 (5.2)	0.39 (0.04)	27 (2.7)
Oxidized (243 K)	10.9 (0.21)		0.9 (0.1)	
Reduced (300 K)	5.4 (0.11)	243 (4.9)	0.45 (0.05)	25 (2.5)

Note. Data in amount adsorbed (μmol/g catalyst) and (μmol/m^2).

Pyridine desorption at similar temperatures from Degussa and anatase TiO_2 suggests similar interactions of both titanias with pyridine, but the areal concentration of the acidic sites is much higher on the Degussa TiO_2. The saturated coverage of pyridine is 5.2 μmol/m^2 on Degussa TiO_2 and 2.7 μmol/m^2 on anatase (Table 3). The saturated coverages of pyridine on each TiO_2 are larger than the saturated coverages of acetone: 4.3 μmol/m^2 on Degussa TiO_2 and 2.2 μmol/m^2 on anatase.

Degussa TiO_2 contains less than 0.5% SiO_2 and Al_2O_3 and a trace amount of Fe_2O_3 (33). Based on the Tanabe model, the addition of both SiO_2 and Al_2O_3 to TiO_2 increases the Brønsted acidity, and the trace amount of Fe_2O_3 forms Lewis acid sites (37). Therefore, these impurities may make Degussa P25 more acidic than anatase TiO_2.

Carbon dioxide desorbs from both TiO_2 samples in two overlapping peaks at 280 and 340 K, as shown in Fig. 12. The high temperature peak is larger for Degussa TiO_2, which also has more total basic sites; the saturated coverages of

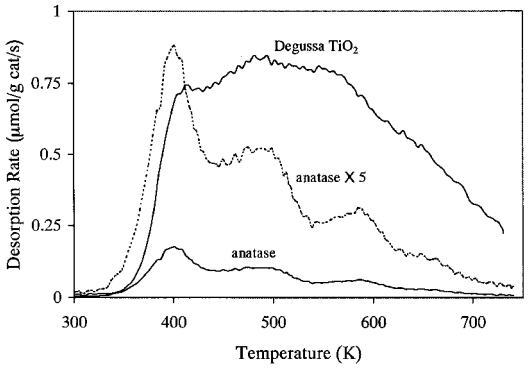

FIG. 11. Temperature-programmed desorption of pyridine on Degussa P25 and anatase TiO_2. The pyridine was adsorbed to saturation coverage at room temperature.

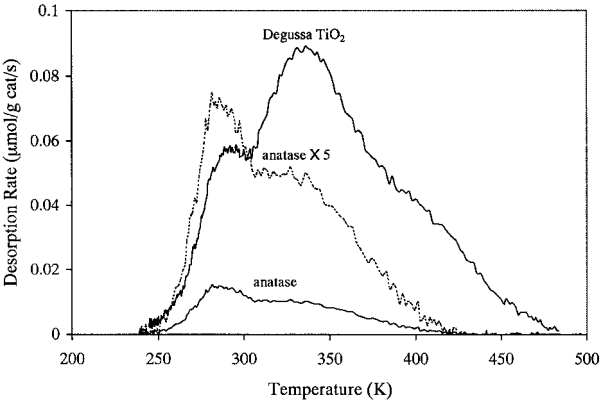

FIG. 12. Temperature-programmed desorption of CO_2 from Degussa P25 and anatase TiO_2. The CO_2 was adsorbed to saturation coverage at 243 K.

CO_2 are 0.21 μmol/m^2 on Degussa TiO_2 and 0.10 μmol/m^2 on anatase TiO_2. Note that the basic site concentration is only about 5% of the acid site concentration.

The amounts of pyridine and CO_2 desorbed, for adsorption at room temperature, are shown in Table 3 for Degussa and anatase TiO_2. The saturated coverages are similar on oxidized and reduced surfaces for a given TiO_2. The small decrease in pyridine coverage when TiO_2 is reduced is consistent with a decrease in acid sites as the oxidation state decreases. Similarly, the increase in CO_2 coverage indicates an increase in basic sites consistent with a decrease in oxidation state. Because CO_2 adsorbs weakly on TiO_2, its saturation coverage at room temperature is less than half of the saturation coverage for adsorption at 243 K.

DISCUSSION

Acetone Condensation Reactions

Aldol condensation and dehydration of acetone (including intramolecular condensation) to form trimethylbenzene does not take place to a large extent on anatase TiO_2, as shown in Table 1. Likewise, Brinkley and Engel (9) detected only acetone desorption during acetone TPD on TiO_2(110) and found no evidence of dissociative adsorption or other reactions of acetone. Similarly, Rekoske and Barteau (42) studied only reductive coupling of acetone on TiO_2. On Degussa TiO_2 (oxidized surface), however, 22% of a monolayer of acetone reacts to form this trimeric condensation product.

Though formation of the cyclic trimer of acetone has not been reported previously for TiO_2, it has been observed on other oxide catalysts. During the continuous reaction of acetone with ZSM-5, acetone formed diacetone alcohol, mesityl oxide, and C_{6+} hydrocarbons at 523 and 561 K, and mesitylene was the sole aromatic species (43). A significant amount of isobutene formed from diacetone cracking and from other mesitylene precursors. Above 561 K, the selectivity to mesitylene declined abruptly, and aromatics such as toluene and xylenes formed. Similarly, during acetone TPD on H-ZSM-5, isobutene, allene, and C_6–C_9 aromatics formed and acetone desorbed, but on Na-ZSM-5, only unreacted acetone desorbed (44). That is, acid sites appear to be necessary for the formation of these condensation products and their secondary reaction products. On ZrO_2, mesitylene was produced from acetone with greater than 70% selectivity in the temperature range 473–673 K, and higher condensation products formed with less than 10% selectivity (20). Isobutene, 2,4,6-trimethylheptatriene-1,3,5 ($C_{10}H_{16}$, a cracking product of the tetrameric condensation product), phorones, and mesityl oxide also formed.

Rekoske and Barteau (42) studied the reaction of acetone on both $TiCl_4$- and TiO_2-derived reagents that were reduced with $LiAlH_4$ and observed carbon–carbon bond formation via carbonyl reductive coupling below 300 K for both liquid and gaseous reactants. First pinacols formed and then 2,3-dimethyl-2-butene.

During the reaction of acetone on MgO and hydrotalcite samples, Garrone *et al.* (4) detected, using UV–vis spectrometry, surface species containing up to five acetone units. During acetaldehyde reaction, species formed that contained more than eight acetaldehyde molecules. For the products with conjugate C=C bonds and carbonyl groups, the species from acetone, e.g., 4,6-dimethylhepta-3,5-dien-2-one, had more methyl branches than the counterparts from acetaldehyde, e.g., hexa-2,4-dienal. Because methyl branches hamper interaction of the molecules with surface sites, they adsorb more weakly through C=C bonds and oxygen and thus are more liable to cyclize and desorb.

Acetaldehyde Reactions

During TPH of acetaldehyde on anatase TiO_2, unreacted acetaldehyde desorbs, and the same products form as reported for other TiO_2 samples (1, 2): crotonaldehyde, butadiene, and butene. However, on Degussa TiO_2, in addition to these products, high-molecular-weight compounds and coke form through further self- or cross-condensations and secondary reactions of condensation products. Crotonaldehyde forms by condensation of two acetaldehyde molecules (2), and further condensation of crotonaldehyde with acetaldehyde forms hexa-2,4-dienal, as shown in Scheme 2. Some hexa-2,4-dienal subsequently reduces to hexa-2,4-dienol. The addition reaction of carbanion to unsaturated bonds (Michael reaction, Scheme 2) may also occur to form branched compounds. However, we did not detect Michael addition products, because either they decompose before they desorb or they undergo further aldolization since they have two carbonyl groups. They could also decompose to form pentene. Further aldolization between the products and acetaldehyde or between the products themselves can form larger molecules that are too strongly bound to desorb from the surface by 723 K. Garrone *et al.* (4) detected condensation product containing up to eight acetaldehyde units on MgO and hydrotalcite.

In addition to polymeric condensation products, alkylbenzenes such as toluene, xylene, and trimethylbenzene also begin to form at 550 K and do not reach maximum rates when heating stops at 723 K. Since adsorbed alkylbenzenes desorb from TiO_2 with peaks near 450 K (15), formation of these alkylbenzenes is reaction-limited. Apparently, they form via the secondary reactions of condensation products, probably through cracking and dehydro-cyclization. Similarly, the coke that remains on the surface after TPH (and is removed by TPO) forms the same way.

Mechanisms

The compounds benzene (C_6H_6) and C_6H_8, which form at 480–490 K during TPH of acetaldehyde, and mesitylene (C_9H_{12}) and C_9H_{14}, which form at 440–490 K during

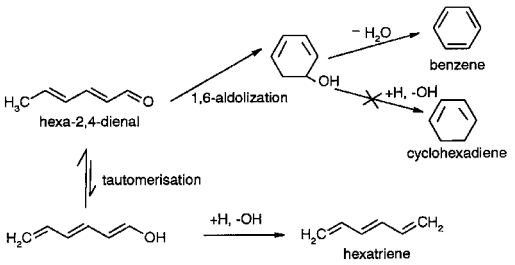

SCHEME 3

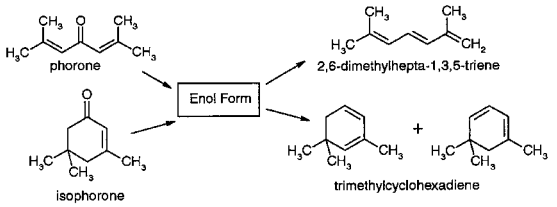

SCHEME 5

TPH of acetone, are apparently produced through secondary reactions of trimeric condensation products. Mesitylene presumably forms via internal 1,6-aldol condensation of 4,6-dimethylhepa-3,5-dien-2-one (18, 20, 29), as shown in Scheme 1. By analogy, benzene forms by condensation of hexa-2,4-dienal (Scheme 3). Deoxygenation can form hexatriene (C_6H_8) and nonatriene (C_9H_{14}), probably through the enol form with H substituting for OH on the surface (Schemes 3 and 4). Cyclohexadiene is not the likely structure for C_6H_8, even though it should also form from dehydroxylation of the 1,6- condensation product; the condensation product is more likely to form benzene (Scheme 3). Phorone or isophorone might also contribute to the formation of C_9H_{14} through reduction of their enol forms, as shown in Scheme 5, but neither phorone nor isophorone was detected during TPD and TPH. The decrease in the amount of mesitylene and the increase in the amount of C_9H_{14} on the reduced surface also supports the formation of C_9H_{14} from the precussor of mesitylene, 4,6-dimethylhepta-3,5-dien-2-one.

The distributions of aromatics and aliphatics in the TPH products of acetone and acetaldehyde are different. During TPH of acetaldehyde, more C_6H_8 forms than C_6H_6, whereas much more C_9H_{12} forms than C_9H_{14} during TPH of acetone. As mentioned above, the methyl branches of long chain condensation products from acetone might hinder the interaction of C=C bonds with surface sites and make these species more weakly bonded. Thus, the adsorbed chain would be more flexible so that the head and tail might contact each other, and this would increase intramolecular condensation (1,6 aldolization). Hexa-2,4-dienal or its enol form, however, bonds strongly with C=C bonds and oxygen, and is apt to desorb after substitution of oxygen with H.

Analogously, butadiene and hexadiene likely form through dehydroxylation of dimeric condensation products of acetaldehyde and acetone, respectively, instead of reductive coupling (Scheme 6). Idriss *et al.* (2) proposed the formation of butene and butadiene via reductive coupling, and Rekoske and Barteau (42) demonstrated carbon–carbon bond formation via carbonyl coupling on a TiO_2 surface reduced with $LiAlH_4$. On reduced surfaces, both butene and butadiene form from acetaldehyde, and hexene and hexadiene form from acetone. However, the alkene peaks for each reactant do not exhibit the same behavior. Moreover, during TPH of acetone on oxidized TiO_2, hexadiene forms but no hexene (Fig. 3). These results suggest that the pair of alkenes (butene and butadiene, hexene and hexadiene) do not form by the same pathway-reductive coupling. The alkenes with one double bond form through reductive coupling, whereas the dienes form from the dimeric condensation products (Scheme 6).

If adsorption is through both the oxygen atom and C=C bonds, the enol should be more stable than the carbonyl form on the surface since it has one more C=C bond. These

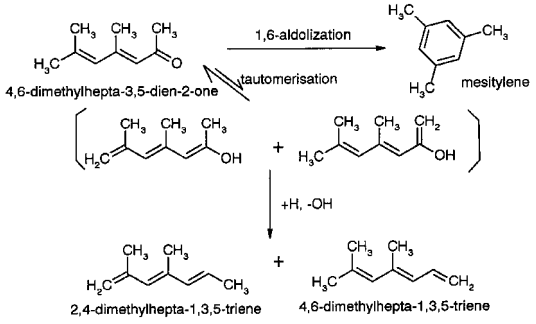

SCHEME 4

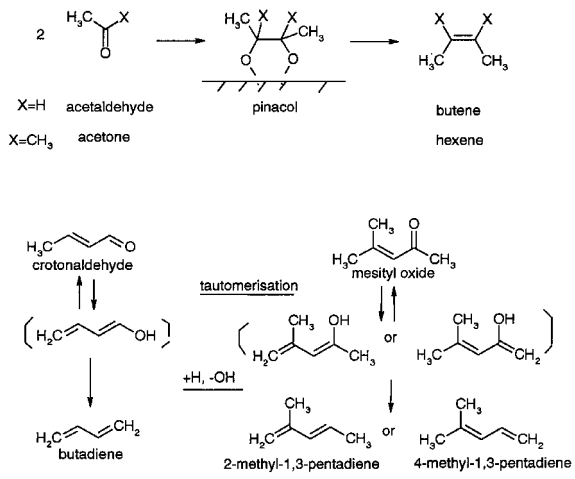

SCHEME 6

enols may exist on the surface as enoxides. At higher temperature, if a hydrogen transfers to the carbonyl carbon, and the oxygen is removed by Ti, then the hydrocarbon with conjugate C=C bonds can desorb. Hexadiene forms in two peaks on the reduced surface. At 410 K, hexadiene forms directly from reduction of mesityl oxide (Scheme 6), which strongly adsorbs on some sites. At high temperature, hexadiene might come from the mesityl oxide that forms by the reverse condensation reaction.

Comparison of Acetone and Acetaldehyde Reactivities

Aldol condensation is strongly susceptible to steric hindrance in the liquid phase (45): whereas most aldehydes with the structure RCH_2CHO readily self-condense, ketone condensations have lower yields. Correspondingly, acetaldehyde conversions are larger than acetone conversions on both TiO_2 surfaces. On Degussa TiO_2, more than 90% of an acetaldehyde monolayer reacts, whereas only about 50% of the acetone monolayer reacts. On anatase TiO_2, 80% conversion of acetaldehyde was reported (2), whereas less than 10% of an acetone monolayer reacts on our anatase TiO_2. The acetaldehyde coverages are approximately twice the acetone coverages on each TiO_2 surface: 370 μmol acetaldehyde/g catalyst and 213 μmol acetone/g catalyst on Degussa TiO_2 versus 50 μmol acetaldehyde/g catalyst and 22 μmol acetone/g catalyst on anatase TiO_2. Higher coverage for acetaldehyde may be partly responsible for its higher reactivity; bimolecular reactions are favored at higher concentrations. The higher coverage for acetaldehyde may also be partially due to the higher reactivity, however; acetaldehyde may undergo condensation reactions during adsorption at room temperature, and this could increase the coverage.

Since more carbon-containing species remain on the surface after TPH of acetaldehyde than after TPH of acetone, acetaldehyde condenses with its condensation products to form larger hydrocarbons at a higher rate than acetone. On Degussa TiO_2, more than 40% of an acetaldehyde monolayer was not removed from the surface during TPH and 67% was not removed during TPD, but only 10% of an acetone monolayer was not removed during TPH and 15% was not removed during TPD. On anatase TiO_2, 4–5% of the acetaldehyde monolayer remained on the surface after either TPH or TPD, but almost no carbon was detected by TPO after acetone TPH.

Formation of Pentene and Pentadiene

Pentadiene and pentene (C_5H_8 and C_5H_{10}) form during TPH of acetaldehyde, and C_5H_8 also forms during TPH of acetone. The unsaturated C_5s must form through secondary reactions of condensation products rather than through direct condensation. Both C_5H_8 and C_5H_{10} form in peaks at 670 K during TPH of acetaldehyde, while hexa-2,4-dienal also desorbs. Pentadiene also forms in a peak at 640 K during TPH of acetone. The relatively high temperatures for their formation suggest that they are likely produced through cracking or decomposition of longer chain compounds.

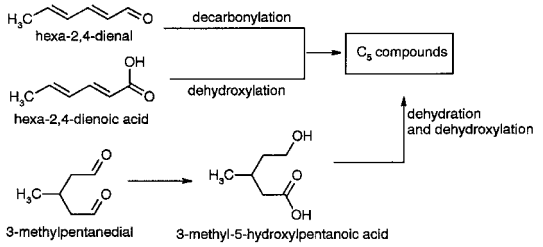

SCHEME 7

Several pathways might lead to the formation of these unsaturated C_5 compounds. As mentioned above, high-molecular-weight compounds form on the surface via further condensation. As the temperature increases, some desorb intact and others crack to smaller molecules, which then desorb. As for isobutene formation from diacetone alcohol or $C_{10}H_{16}$ from $C_{12}H_{20}O_2$, cracking is accompanied by the formation of acetic acid (20).

The Michael addition product of crotonaldehyde and acetaldehyde, 3-methylpentanedial (Scheme 7), might also be a precursor to C_5 compounds, but it was not detected in the gas phase. It could undergo intermolecular disproportionation, dehydration, decarboxylation, and possible rearrangement to form pentene, as shown in Scheme 7.

The C_5 compounds have a higher peak temperature but desorb while hexa-2,4-dienal desorbs and therefore might form from strongly adsorbed hexa-2,4-dienal. This is analogous to the formation of furan from furfural (46):

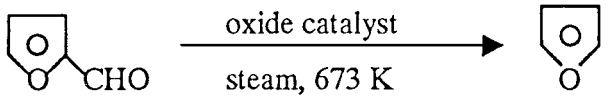

furfural furan

The C_5 compounds might also form following decarboxylation of hexa-2,4-dienoic acid,

$$CH_3CH{=}CHCH{=}CHCOOH$$
$$\rightarrow CH_3CH{=}CHCH{=}CH_2 + CO + [O],$$

which is formed from oxidation or disproportionation of hexa-2,4-dienal, similar to acetic acid decomposition to CH_4 on reduced TiO_2(001) (47):

$$CH_3COOH \rightarrow CH_4 + CO + [O].$$

Pentadiene forms in a peak around 650 K during TPH of acetone on both oxidized and reduced TiO_2. Analogous

to the cracking of diacetone alcohol and mesityl oxide to isobutene (20, 29), C_5H_8 might form from cracking and rearrangement of 4,4-dimethyl hepta-2,6-dione.

Comparison of Degussa and Anatase TiO_2

The saturation coverages of acetone and acetaldehyde per m^2 on Degussa TiO_2 are about twice those on anatase. The higher concentration is expected to favor bimolecular reactions such as condensation and reductive coupling on Degussa TiO_2. In addition, the acidic (or basic) site concentration per m^2, as measured by pyridine (or CO_2) TPD, is twice as high on Degussa. Since both acidic and basic sites participate in catalyzing condensation reactions, Degussa TiO_2 is also expected to exhibit higher rates for these reactions. Indeed, on Degussa TiO_2, about 35% of an acetone monolayer forms mesitylene and alkenes, whereas on anatase, less than 5% does. Also on Degussa TiO_2, almost 10 times as many carbon containing species per m^2 (>40% of a monolayer) remain after TPH of acetaldehyde than on anatase TiO_2 (4–5%), and almost 5 times as many remain on Degussa TiO_2 after TPH of acetone. In addition, on anatase TiO_2, acetaldehyde mainly desorbs intact or as the dimeric condensation product, and no compounds larger than crotonaldehyde are observed. In contrast, on Degussa TiO_2, acetaldehyde mostly undergoes further aldol condensation to form C_4+ (including butene and butadiene) compounds and coke at higher temperature.

Salvapati *et al.* (29) pointed out that acidic catalysts, high temperatures, and high pressures favor the formation of mesitylene from acetone on various oxide surfaces, though they did not report this reaction on TiO_2. Lippert *et al.* (20) also showed that the catalyst and reaction conditions significantly affect acetone condensation. Similarly for acetaldehyde, Idriss *et al.* (1, 2) reported different conversions and selectivities for anatase and for TiO_2(001) pretreated in different conditions. Since CO_2 is weakly adsorbed and 20 times as much pyridine adsorbs, and since pyridine is relatively strongly adsorbed, titania has more acid sites. Mesitylene was the main product from acetone on ZrO_2 with selectivities of 72–79% (20). If the acid–base characteristics of TiO_2 are similar to those of ZrO_2 (since they both are in the IVB column), mesitylene might be expected to be selectively produced on TiO_2. As described above, the acetone and pyridine surface concentrations are similar for each TiO_2, as might be expected if they adsorb on the same sites.

Oxidized versus Reduced TiO_2

As shown in Fig. 5, heating oxidized TiO_2 in H_2 forms water above 600 K as the surface is reduced; water does not form at this temperature on reduced TiO_2. This amount of water corresponds to removal of 2.5 oxygen atoms/nm^2 from Degussa TiO_2 (209 μmol/g), and 4.2 oxygen atoms/nm^2 from anatase TiO_2 (70 μmol/g). Since the oxidized surface does not appear to start to reduce until 600 K, products that form below 600 K during TPH apparently form on an oxidized surface. Since acetone TPD and TPH spectra are similar on Degussa TiO_2, with the main difference being less species remaining on the surface after TPH, the only possible effect of reduction above 600 K would be to increase the rate of formation of alkenes, which desorb from the surface.

Idriss *et al.* (1) observed a significant change in the selectivity for acetaldehyde reactions on TiO_2 as the degree of reduction of their single crystal was changed by sputtering and then annealing at different temperatures. They concluded that condensation and coupling reactions exhibit important but opposite dependencies on surface reduction. Whereas reduced surfaces were active for coupling to form butene due to the presence of oxygen vacancies, oxidized surfaces were active for self-condensation of acetaldehyde to crotonaldehyde or crotyl alcohol due to the abundance of oxide anions (acting as Lewis base sites). On both oxidized and reduced Degussa TiO_2, acetone undergoes aldol condensation and dehydration, followed by cyclization (internal aldolization) to form mesitylene. As shown in Table 1, the amounts of mesitylene formed on both oxidized and reduced Degussa surfaces are essentially identical. However, hexene formed only on reduced TiO_2. This confirms the suggestion by Rekoske and Barteau (42) that 2,3-methyl-2-butene (hexene) forms through reductive coupling of two acetone molecules. Two molecules of acetone first form a surface pinacolate intermediate via reductive dimerization, and then the dimer forms hexene by deoxygenation, as shown in Scheme 6.

The selectivities for hexadiene and hexene formation from acetone increase dramatically on the reduced Degussa TiO_2 surface (Table 1). More C_9H_{14} also forms on reduced TiO_2. Hexadiene and C_9H_{14} may form by reduction of dimeric and trimeric condensation products rather than by reductive coupling, as shown in Schemes 4 and 6. Presumably, oxygen vacancies are important in removing oxygen from surface species to form unsaturated hydrocarbons. More CO_2 and CO form on the oxidized surface because more oxygen is available to oxidize the hydrocarbons than on the reduced surface.

Significance for Photocatalysis

Acetone and acetaldehyde form as intermediates during PCO of 2-propanol and ethanol, respectively (7, 8, 10), and in addition, they are pollutants that can be oxidized by PCO (10, 12, 13, 16, 17). Thus, acetone and acetaldehyde are present in significant surface coverages during some PCO reactions. As shown in Fig. 1, mesitylene starts desorbing from TiO_2 at 400 K and it is desorption limited. This means mesitylene forms between 300 and 400 K while the acetone coverage is still high. Thus, the rate of mesitylene formation at 300 K could be significant during PCO

at room temperature. Similarly, acetaldehyde forms crotonaldehyde by 400 K, which indicates that acetaldehyde condensation products also form at relatively low temperature.

Since aromatics have much lower PCO rates than alcohols, aldehydes, or ketones (15), these condensation reactions can cover the TiO_2 surface with less reactive species and poison PCO. This poisoning would be expected to be more important at elevated temperature. Indeed, during acetaldehyde PCO on Degussa TiO_2, the PCO rate reached a steady state at room temperature. At 363 K, however, the catalyst rapidly deactivated (13), presumably because condensation products formed faster at 363 K than they could be oxidized. Thus, for PCO of reaction mixtures that contain acetone or acetaldehyde or contain reactants that can form these as intermediates, condensation reactions at elevated temperature may be responsible or partly responsible for deactivation. Both H_2O and O_2 are present during PCO, and they may affect the TiO_2 surface and the condensation reactions, but these effects were not looked at in the current study. Though PCO is typically run at room temperature and that is one of its advantages, often the catalyst temperature is higher because of heating by the lamps or by solar radiation used to obtain the UV radiation. The higher temperature may not be an advantage, however, because of the increased rates of condensation reactions.

CONCLUSIONS

Acetaldehyde and acetone both undergo condensation reactions on TiO_2, and Degussa P25 TiO_2 is a much more active catalyst for condensation than anatase TiO_2. Approximately 20% of a monolayer of acetone forms the trimeric condensation product mesitylene on Degussa TiO_2; only 1.4% of a monolayer forms mesitylene on anatase. Both the higher surface concentration of acetone and the higher concentration of acidic and basic sites on Degussa TiO_2 favor condensation reactions. Similarly, Degussa TiO_2 is a better catalyst for acetaldehyde condensation reactions to form longer chain molecules and coke.

Reductive coupling of acetaldehyde or acetone forms butene or hexene. The reduced surface is more active for reductive coupling because it contains more oxygen vacancies, which are necessary for the formation of surface pinacolate intermediates.

Secondary reactions of aldol condensation products form unsaturated aliphatic hydrocarbons such as C_4H_8, C_5H_8, C_5H_{10}, C_6H_8, C_6H_{10}, C_9H_{14}, and $C_{10}H_{16}$. Dehydroxylation forms C_4H_6, C_6H_8, C_6H_{10}, and C_9H_{14}, and cracking, decarbonylation, or decarboxylation form C_4H_8, C_5H_8, C_5H_{10}, and $C_{10}H_{16}$. Since dehydroxylation also prefers a reductive environment, the selectivity for the products formed through this reaction increases dramatically with reduction of the surface. Acetaldehyde is more reactive than acetone for oligomer formation on each TiO_2, and this is attributed to the higher surface concentrations of acetaldehyde and less steric hindrances with acetaldehyde and its condensation products than with acetone and its condensation products.

ACKNOWLEDGMENTS

We gratefully acknowledge support by the National Science Foundation, Grant CTS-9714403. We also thank Professor Mark A. Barteau of the University of Delaware for providing us the TiO_2 anatase sample and his manuscripts prior to publication and for his valuable suggestions.

REFERENCES

1. Idriss, H., and Barteau, M. A., *Catal. Lett.* **40**, 147 (1996).
2. Idriss, H., Kim, K. S., and Barteau, M. A., *J. Catal.* **139**, 119 (1993).
3. Idriss, H., Diagne, C., Hindermann, J. P., Kiennemann, A., and Barteau, M. A., *J. Catal.* **155**, 219 (1995).
4. Garrone, E., Bartalini, D., Coluccia, S., Martra, G., Tichit, D., and Figueras, F., *Studies Surf. Sci. Catal.* **90**, 183 (1994).
5. Luo S., and Falconer, J. L., *Catal. Lett.* **57**, 89 (1999).
6. Rekoske, J.E., Ph.D. dissertation, Univ. of Delaware, 1998.
7. Muggli, D. S., McCue, J. T., and Falconer, J. L., *J. Catal.* **173**, 470 (1998).
8. Larson, S. A., Widegren, J. A., and Falconer, J. L., *J. Catal.* **157**, 611 (1995).
9. Brinkley, D., and Engel, T., *J. Phys. Chem. B* **102**, 7596 (1998).
10. Muggli, D. S., and Falconer, J. L., *J. Catal.* **175**, 213 (1998).
11. Sauer, M. L., and Ollis, D. F., *J. Catal.* **158**, 570 (1996).
12. Kennedy III, J. C., and Datye, A. K., *J. Catal.* **179**, 375 (1998).
13. Falconer, J. L., and Magrini-Bair, K. A., *J. Catal.* **179**, 171 (1998).
14. Muggli, D. S., Larson, S. A., and Falconer, J. L., *J. Phys. Chem.* **100**, 15886 (1996).
15. Larson, S. A., and Falconer, J. L., *Catal. Lett.* **44**, 57 (1997).
16. Pearl J., and Ollis, D. F., *J. Catal.* **136**, 554 (1992).
17. Raupp, G. B., and Junio, C. T., *Appl. Surf. Sci.* **72**, 321 (1993).
18. Reichle, W. T., *J. Catal.* **63**, 295 (1980).
19. Reichle, W. T., *Chemtech.* **11**, 698 (1981).
20. Lippert, S., Baumann, W., and Thomke, K., *J. Mol. Catal.* **69**, 199 (1991).
21. Haffad, D., Kameswari, U., Bettahar, M. M., Chambellan, A., and Lavalley, J. C., *J. Catal.* **172**, 85 (1997).
22. Koutstaal C. A., and Ponec, V., *Studies Surf. Sci. Catal.* **92**, 105 (1994).
23. Di Cosimo J. I., and Apesteguia, C. R., *J. Mol. Catal.* **130**, 177 (1998).
24. Choudhary, Y. R., Mulla, S. A. R., and Rane, V. H., *J. Chem. Technol. Biotechnol.* **72**, 125 (1998).
25. Rochester, C. H., and Smith, D. G., *J. Chem. Soc. Faraday Trans.* **82**, 2569 (1986).
26. Podrebarac, G. G., Ng, F. T. T., and Rempel, G. L., *Chem. Eng. Sci.* **52**, 2991 (1997).
27. Podrebarac, G. G., Ng, F. T. T., and Rempel, G. L., *Chem. Eng. Sci.* **53**, 1067 (1998).
28. Podrebarac, G. G., Ng, F. T. T., and Rempel, G. L., *Chem. Eng. Sci.* **53**, 1077 (1998).
29. Salvapati, G. S., Ramanamurty, K. V., and Janardanarao, M., *J. Mol. Catal.* **54**, 9 (1989).
30. Novakova, J., Kubelkova, L., and Dolejsek, Z., *J. Mol. Catal.* **30**, 185 (1987).

31. Zhang, G., Hattori, H., and Tanabe, K., *Appl. Catal.* **36**, 189 (1988).
32. Zhang, G., Hattori, H., and Tanabe, K., *Appl. Catal.* **40**, 183 (1988).
33. Nargiello, M., and Herz, T., *in* "Photocatalytic Purification and Treatment of Water and Air" (D. F. Ollis and H. Al-Ekabi, Eds.), p. 169. Elsevier Science, Amsterdam, 1993.
34. Larson, S. A., and Falconer, J. L., *Appl. Catal. B* **4**, 325 (1994).
35. Kim, K. S., and Barteau, M. A., *Langmuir* **4**, 533 (1988).
36. Haerudin, H., Bertel, S., and Kramer, R., *J. Chem. Soc. Faraday Trans.* **94**, 1481 (1998).
37. Matsuda, S., and Kato, A., *Appl. Catal.* **8**, 149 (1983).
38. Scherzer, J., and Gruia, A. J., "Hydrocracking Science and Technology." Dekker, New York, 1996.
39. Parrilo, D. J., Adamo, A. T., Kokotailo, G. T., and Gorte, R. J., *Appl. Catal.* **67**, 107 (1990).
40. Parfitt, G. D., Ramsbotham, J., and Rochester, C. H., *Trans. Faraday Soc.* **67**, 1500 (1971).
41. Graham, J., Rudham, R., and Rochester, C. H., *J. Chem. Soc. Faraday Trans.* **79**, 2991 (1983).
42. Rekoske, J. E., and Barteau, M. A., *Ind. Eng. Chem. Res.* **34**, 2931 (1995).
43. Chang, C. D., and Silvestri, A. J., *J. Catal.* **47**, 249 (1977).
44. Novakova, J., Kubelkova, L., and Dolejsek, *J. Mol. Catal.* **39**, 195 (1987).
45. Gutsche, C. D., "The Chemistry of Carbonyl Compounds." Prentice-Hall, Englewood Cliffs, NJ, 1967.
46. Morrison, R. T., and Boyd, R. N., "Organic Chemistry." 6th ed. Prentice-Hall, Englewood Cliffs, NJ, 1992.
47. Kim, K. S., and Barteau, M. A., *J. Catal.* **125**, 353 (1990).